EUROPHYSICS LETTERS 15 August 2005

Europhys. Lett., **71** (4), pp. 692–698 (2005)
DOI: 10.1209/epl/i2005-10127-x

Self-diffusion of rod-like viruses in the nematic phase

M. P. Lettinga[1], E. Barry[2] and Z. Dogic[2]

[1] *IFF, Institut Weiche Materie, Forschungszentrum Jülich - D-52425 Jülich, Germany*
[2] *Rowland Institute at Harvard, Harvard University - Cambridge, MA 02142, USA*

received 21 March 2005; accepted 17 June 2005
published online 22 July 2005

PACS. 82.70.-y – Disperse systems; complex fluids.
PACS. 61.30.-v – Liquid crystals.
PACS. 66.10.-x – Diffusion and ionic conduction in liquids.

Abstract. – We measure the self-diffusion of colloidal rod-like virus fd in an isotropic and nematic phase. A low-volume fraction of viruses are labelled with a fluorescent dye and dissolved in a background of unlabelled rods. The trajectories of individual rods are visualized using fluorescence microscopy from which the diffusion constant is extracted. The diffusion parallel ($D_\parallel$) and perpendicular ($D_\perp$) to the nematic director is measured. The ratio ($D_\parallel/D_\perp$) increases monotonically with increasing virus concentration. Crossing the isotropic-nematic phase boundary results in increase of $D_\parallel$ and decrease of $D_\perp$ when compared to the diffusion in the isotropic phase ($D_{\rm iso}$).

Introduction. – Suspensions of semi-flexible polymers exhibit a variety of dynamical phenomena, of great importance to both physics and biology, that are still only partially understood. Advances over the past decade include direct visual evidence for a reptation-like diffusion of polymers in a highly entangled isotropic solution and shape anisotropy of an isolated polymer [1–4]. If the concentration of the polymers is increased, a suspension undergoes a first-order phase transition to a nematic phase, which has long-range orientational order but no long-range positional order. As a result of the broken orientational symmetry, it is expected that the diffusion of polymers in the nematic liquid crystals will be drastically different from that in concentrated isotropic solutions. While the static phase behavior of semi-flexible nematic polymers is well understood in terms of the Onsager theory and its extensions by Khoklov and Semenov [5, 6], the dynamics of semi-flexible polymers in the nematic phase is much less explored [7].

In this paper, we determine the concentration dependence of the anisotropic diffusion of semi-flexible viruses in a nematic phase and compare it to the diffusion in the isotropic phase. Experimentally, the only data on the translational diffusion of colloidal rods in the nematic phase was taken in a mixture of labelled and unlabelled polydysperse boehmite rods using fluorescence recovery after photobleaching (FRAP) [8]. Theoretically, molecular-dynamics simulations were performed on hard spherocylinder and ellipsoidal systems from which the anisotropic diffusion data was extracted [9–11]. The unisotropic diffusion has also been studied in low-molecular-weight thermotropic liquid crystals using NMR spectroscopy or inelastic scattering of neutrons [12].

Real-space microscopy is a powerful method that can reveal dynamics of colloidal and polymeric liquid systems that are inaccessible to other traditional techniques [3,7]. We use digital microscopy to directly visualize the dynamics of fluorescently labelled fd in a nematic background of unlabelled fd. The advantage of this method is an easy interpretation of data and no need to obtain macroscopically aligned monodomains in magnetic fields. The advantages of using fd are its large contour length which can be easily visualized with optical microscope and its phase behavior which can be quantitatively described with the Onsager theory extended to account for electrostatic repulsive interactions and semi-flexibility [13,14]. Viruses such as fd and TMV have been used earlier to study the rod dynamics in the isotropic phase [15].

Experimental methods. – The physical characteristics of the bacteriophage fd are its length $L = 880\,\mathrm{nm}$, diameter $D = 6.6\,\mathrm{nm}$, persistence length of 2200 nm and a surface charge of $10\,\mathrm{e}^-/\mathrm{nm}$ at pH 8.2 [16]. Bacteriophage fd suspension forms isotropic, cholesteric and smectic phases with increasing concentration [16–18]. The free energy difference between the cholesteric and nematic phase is very small and locally the cholesteric phase is identical to nematic. We expect that at short time scales the diffusion of the rods for these two cases would be the same. Hereafter, we refer to the liquid crystalline phase at intermediate concentration as a nematic instead of a cholesteric.

The fd virus was prepared according to a standard biological protocol using XL1-Blue strain of *E. coli* as the host bacteria [19]. The yields are approximately 50 mg of fd per liter of infected bacteria and the virus is typically grown in 6 liter batches. Subsequently, the virus is purified by repetitive centrifugation (108000 g for 5 hours) and re-dispersed in a 20 mM phosphate buffer at pH = 7.5. First-order isotropic-nematic (I-N) phase transition for fd under these conditions takes place at a rod concentration of 15.5 mg/ml.

Fluorescently labelled fd viruses were prepared by mixing 1 mg of fd with 1 mg of succinimidyl ester Alexa-488 (Molecular Probes) for 1 hour. The dye reacts with free amine groups on the virus surface to form irreversible covalent bonds. The reaction is carried out in small volume (100 μl, 100 mM phosphate buffer, pH = 8.0) to ensure a high degree of labelling. Excess dye was removed by repeated centrifugation steps. Absorbance spectroscopy indicates that there are approximately 300 dye molecules per each fd virus. Viruses labelled with fluorescein isothiocynante, a dye very similar to Alexa 488, exhibit the phase behavior identical to that of unlabelled virus. Since liquid crystalline phase behavior is a sensitive test of interaction potential, it is reasonable to assume that the interaction potential between labelled viruses is very similar to that between unlabelled viruses.

The samples were prepared by mixing one unit of anti-oxygen solution (2 mg/ml glucose oxidase, 0.35 mg/ml catalase, 30 mg/ml glucose and 5% β-mercaptoethanol), one unit of a dilute dispersion of Alexa 488 labelled viruses and eight units of the concentrated fd virus suspension at the desired concentration. Under these conditions the fluorescently labelled viruses are relatively photostable and it is possible to continuously observe rods for 3-5 minutes without significant photobleaching. The ratio of labelled to unlabelled particles is roughly kept at 1 : 30000. The samples were prepared by placing 4 μl of solution between a No 1.5 cover slip and coverslide. The thickness of the samples is about 10 μm. Thin samples are important to reduce the signal of out-of-focus particles. Samples are equilibrated for half an hour, allowing flows to subside and liquid crystalline defects to anneal. We have analyzed data at various distances from the wall and have not been able to observe a significant influence of wall on the diffusion of viruses.

For imaging we used an inverted Nikon TE-2000 microscope equipped with 100×1.4 NA PlanApo oil immersion objective, a 100 W mercury lamp and a fluorescence cube for Alexa 488 fluorescent dye. The images where taken with a cooled CCD Camera (CoolSnap HQ,

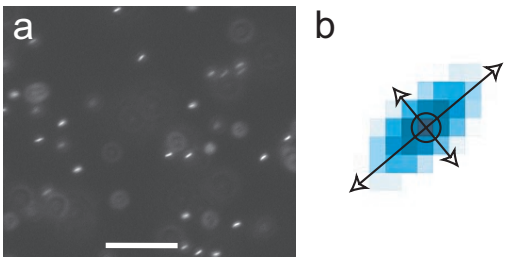

Fig. 1 – (a) Image of fluorescently labelled rods dissolved in a background nematic phase of unlabelled rods. The scale bar is 5 μm. (b) Two-dimensional Gaussian fit to an individual rod. Arrows indicate the long and short axis. The circle indicates the center of mass. From this fit it is possible to obtain the orientation of an individual fd rod. The pixel size is 129 nm.

Roper Scientific) set to an exposure time of 60 ms, running in a overlap mode at a rate of 16 frames per second with 2×2 binning. The pixel size was 129 nm and the field of view was 89 μm $\times$ 66 μm. Typically there were around hundred fluorescently labelled rods in the field of view. For each fd concentration ten sequences of four hundred images were recorded.

Analysis method. – Figure 1a shows a typical image of fluorescently labelled rods in a background nematic of unlabelled rods. Due to limited spatial and temporal resolution of the optical microscope, labelled fd appear as a slightly anisotropic rod, although the actual aspect ratio is larger than 100. To measure the anisotropic diffusion in the nematic phase, it is first necessary to determine the nematic director which has to be uniform within a field of view. Spatial distortion of the nematic would significantly affect our results. The centers of mass and orientation of rods are obtained sequentially. In a first step, a smoothed image is used to identify the rods and obtain the coordinates of its center of mass using image processing code written in IDL [20]. Subsequently, a two-dimensional Gaussian fit around the center of mass of each rod is performed (fig. 1b). From this fit the orientation of each rod-like virus is obtained. This procedure is then repeated for a sequence of images.

The length of a trajectory is usually limited to a few seconds, after which the particles diffuse out of focus. In fig. 2a and b we plot the trajectories of an ensemble of particles for both isotropic and nematic sample. As expected, the trajectories in the isotropic phase are spherically symmetric (fig. 2a) while those in the nematic phase exhibit a pronounced anisotropy (fig. 2a). The symmetric nature of the distribution indicates that there is no drift or flow in our samples. We obtain the orientation of the nematic director using two independent methods. One method is to measure the main axis of the distribution shown in fig. 2b. This procedure assumes that the diffusion is largest along the nematic director. An alternative method is to plot a histogram of rod orientations which are obtained from 2D Gaussian fits to each rod (fig. 1b). The resulting orientational distribution function (ODF) is shown in fig. 2c. In principle, it should be possible to obtain both the nematic director and order parameter from ODF shown in fig. 2c. We find that the order parameter obtained in such a way is systematically higher than the order parameter obtained from more reliable X-ray experiments [14]. This is due to significant rotational diffusion each rod undergoes during an exposure time of 60 ms.

The differences in the orientation of the nematic director obtained using these two methods is always less than 5 degrees. For the example shown in fig. 2, from the anisotropy of the diffusion we obtain a nematic director at an angle of 31.2° (fig. 2b), while the peak of the orientational distribution function lies at 30.2° (fig. 2c). The director can be "placed" along

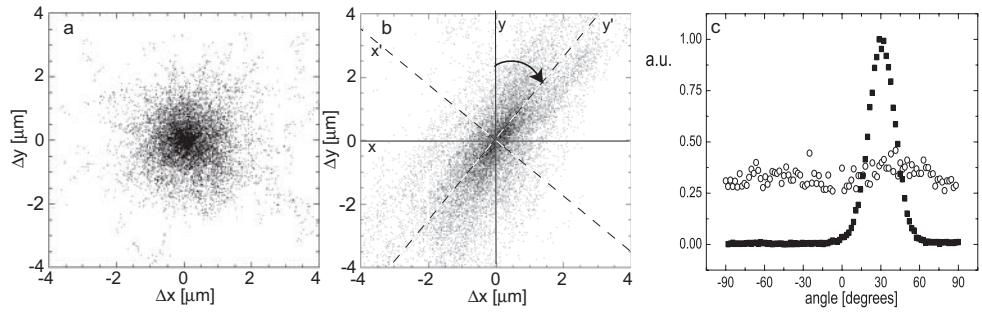

Fig. 2 – (a) A collection of trajectories of fluorescently labelled virus particles in the isotropic phase. All trajectories are translated so that the first point is located at the origin. For clarity we only show the center of mass and not the line connecting subsequent points in a particle trajectory. The concentration of virus in this sample was 14 mg/ml. (b) Anisotropic trajectories of the fluorescently labelled viruses diffusing in the nematic phase. The concentration of the background virus in this sample was 21 mg/ml. x' and y' indicate a new lab-frame in which the director is aligned along the y'-axis. (c) The orientational distribution function obtained by plotting the probability distribution function of the virus orientation for isotropic (open circles) and nematic phase (full squares). The orientation of the virus is obtained from two-dimensional Gaussian fits, an example of which is shown in fig. 1b. The nematic directors obtained from (b) and (c) are almost identical.

one of the two main axes by rotating the lab-frame.

The diffusion coefficients of the rods parallel ($D_{\parallel}$) and perpendicular ($D_{\perp}$) to the director are calculated from the x'- and y'-component of the mean-square displacement. When the director lies along the y'-axis, $D_{\parallel}$ and $D_{\perp}$ are given by

$$D_{\parallel} = \frac{1}{N}\frac{1}{2}\sum\{y_i'(t) - y_i'(0)\}^2, \tag{1}$$

$$D_{\perp} = \frac{1}{N}\frac{1}{\sqrt{2}}\sum\{x_i'(t) - x_i'(0)\}^2, \tag{2}$$

where N is the number of traced particles. To obtain $D_{\perp}$, D_x is multiplied with $\sqrt{2}$ since only one component of the diffusion perpendicular to the director is measured. The underlying assumption of our analysis is that the nematic director is oriented in the field of view. For 10 μm thin samples this is reasonable.

Results and discussion. – Typical mean-square displacements (MSD) are shown in fig. 3 for samples in an isotropic and nematic phase. On average, the mean-square displacement was linear over fifty frames in the nematic phase, but only over twenty-five frames in the isotropic phase. The diffusion perpendicular to the director is slower in the nematic phase as compared to the isotropic phase. Therefore in the nematic phase, the particles stay longer in focus and can be tracked for a longer time. Because the MSDs are linear over the entire time range and displacements are up to a few times the particle length, we are measuring pure long-time self-diffusion. Visual inspection of the trajectories in the concentrated isotropic phase, just below I-N coexistence shows no characteristics of the reptation observed in suspensions of long DNA fragments or actin filaments [2, 3]. This points to the fact that fd is very weakly entangled in a concentrated isotropic suspension. This is in agreement with recent microrheology measurements of fd suspensions [21]. We note that MSDs obtained from few hundred trajectories within a single field of view are very accurate. However, if we move to

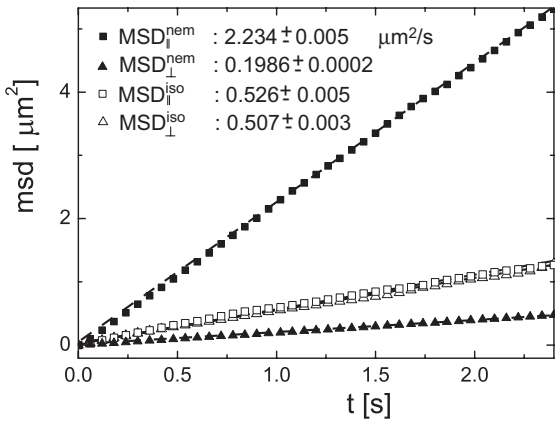

Fig. 3 – The mean-square displacements of rods along the director (full squares) and perpendicular to the director (full triangles) obtained for a nematic sample at virus concentration of 21 mg/ml. The isotropic data are given by the open squares and were taken just below the I-N phase transition at virus concentration of 14 mg/ml. The diffusion along the director is significantly enhanced when compared to the diffusion in the isotropic phase, while the diffusion perpendicular to the director is significantly suppressed. The mean-square displacements shown in this figure are measured from a single field of view.

another region of the sample we obtain MSD with a slightly different slope. This leads to the conclusion that the largest source of error in measuring the anisotropic diffusion coefficient is the uniformity of the nematic director within the field of view.

The concentration dependence of the anisotropic diffusion constants is shown in fig. 4a. The nematic phase melts into an isotropic phase at low concentrations and freezes into a

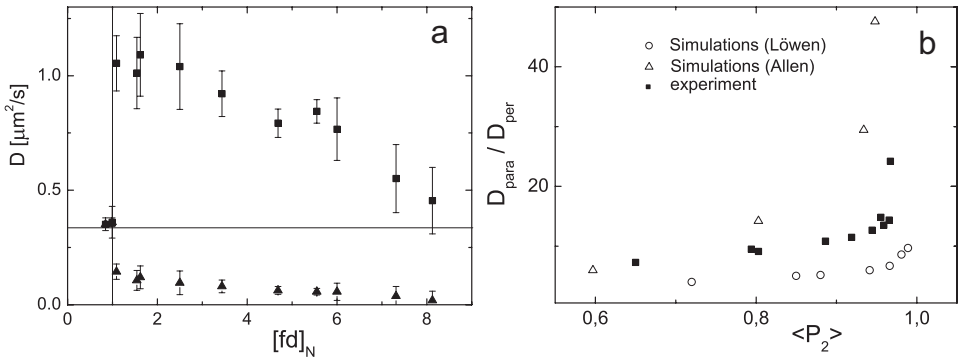

Fig. 4 – (a) The concentration dependence of the translational diffusion parallel to ($D_\parallel$) and perpendicular to ($D_\perp$) the nematic director are indicated by squares and triangles, respectively. The nematic phase in coexistence with the isotropic phase occurs at $c_{fd} = 15.5\,\mathrm{mg/ml}$ and is indicated by a vertical line. The x-axis is rescaled so that I-N transition takes place at $[fd]_N$=1. (b) The plot of the dimensionless ratio of the parallel to perpendicular diffusion constant $D_\parallel/D_\perp$ as a function of the nematic order parameter. The concentration dependence of the nematic order parameter is taken from ref. [14]. Open triangles are data for hard spherocylinders with aspect ratio of 10 taken from ref. [11] while open circles are data for ellipsoids with aspect ratio 10 taken from [9].

smectic phase at high concentrations. We made an attempt to measure the diffusion of rods in the smectic phase, but have not seen any appreciable diffusion on optical length scales over a time period of minutes. The most strinking feature of our data is a strong discontinuity in the behavior of the diffusion constant at the I-N phase transition. Compared to diffusions in isotropic case $D_{\rm iso}$, $D_{\parallel}$ is larger by a factor of four, while $D_{\perp}$ is smaller by a factor of two. The concentration dependence of $D_{\parallel}$ and $D_{\perp}$ exhibit different behavior. With increasing concentration, for $D_{\parallel}$ we measure an initial plateau, which is followed by a broad region where the diffusion rate decreases monotonically. $D_{\perp}$, however, shows a monotonic decrease of the diffusion constant over the whole concentration range where nematic phase is stable.

It is useful to compare our results to previous theoretical and experimental work, especially the measurements of the diffusion coefficient for silica-coated boehmite rods [8]. In this work the authors measure $D_{\parallel}/D_{\perp} \approx 2$ for monodomain nematic samples which are in coexistence with the isotropic phase. This is significantly different from $D_{\parallel}/D_{\perp} \approx 7.5$ for fd virus. Another significant difference is that results on boehmite indicate that both $D_{\parallel}$ and $D_{\perp}$ are smaller than $D_{\rm iso}$, in contrast to our measurements, where $D_{\parallel}$ is much larger and $D_{\perp}$ is much smaller than $D_{\rm iso}$.

When comparing our data to simulations of the diffusion of hard spherocylinders and ellipsoids [9,11], one needs to compare equivalent samples. Scaling to rod concentration where the I-N transition takes place would be erroneous, since fd virus is a semi-flexible rod. The semi-flexibility of the virus drives the isotropic-nematic phase transition to higher concentrations and it significantly decreases the order parameter of the nematic phase in coexistence with the isotropic phase [13,14]. We choose to compare data and simulations at the same value of the nematic order parameter which is determined independently [14]. For fd, the nematic order parameter is 0.65 at the I-N coexistence, it monotonically increases with increasing rod concentration and saturates at high rod concentration. Experiment and simulation qualitatively agree and both show a rapid increase of $D_{\parallel}/D_{\perp}$ ratio with increasing nematic order parameter (fig. 4b). We note that there is a discrepancy between the simulations results obtained in refs. [9,11] which might be due to different systems studied in these two papers.

Interestingly, simulations predict that upon increasing rod concentration beyond I-N coexistence $D_{\parallel}$ initially increases and subsequently upon approaching the smectic phase decreases. The author argues that the non-monotonic behavior of $D_{\parallel}$ is the result of the interplay between two effects. First, with increasing rod concentration the nematic order parameter increases which enhances $D_{\parallel}$. Second, with increasing rod concentration there is less free volume which leads to decrease of $D_{\parallel}$. The author further argues that the first effect dominates at low rod concentrations where the nematic order parameter rapidly increases while the second effect dominates at high rod concentrations where the nematic order parameter is almost saturated. In contrast, both of these effects contribute to a monotonic decrease in $D_{\perp}$ with increasing concentration, which is observed in simulations. Due to relatively large error in our experimental data, it is not clear if the behavior of $D_{\parallel}$ is non-monotonic. There is an initial hesitation, but $D_{\parallel}$ decreases over most of the concentration range. This difference between simulations and experiment might be because we compare experiments of semi-flexible fd to simulations of perfectly rigid rods. Compared to semi-flexible rods, the order parameter of rigid rods increases much faster with increasing rod concentration [14].

It would be of interest to extend our measurements to rotational diffusion in the isotropic and nematic phase. At present the rod undergoes significant rotational diffusion during each exposure which reduces resolution and prevents accurate determination of the instantaneous orientation of a rod. It might be possible to significantly reduce the exposure time by either using a more sensitive CCD camera or a more intense laser as an illumination source.

Conclusions. – Using fluorescence microscopy we have visualized rod-like viruses and measured the anisotropic long-time self-diffusion coefficients in the isotropic and nematic phase. In the nematic phase the diffusion along the director and the diffusion perpendicular to the director decrease monotonically with increasing rod concentration. The ratio of parallel to perpendicular diffusion increases monotonically with increasing rod concentration. The results compare qualitatively with simulations on hard rods with moderate aspect ratios.

Note added in proofs. – Our experiments coupled with recent observations of sub-diffusive behavior of ellipsoidal particles in a nematic fd illustrate that much remains to be understood about the dynamics of colloidal liquid crystals [22].

* * *

PL is supported in part by Transregio SFB TR6, "Physics of colloidal dispersions in external fields". ZD is supported by a Junior Fellowship from Rowland Institute at Harvard.

REFERENCES

[1] Perkins T. T., Smith D. E. and Chu S., *Science*, **264** (1994) 819.
[2] Smith D. E., Perkins T. T. and Chu S., *Phys. Rev. Lett.*, **75** (1995) 4146.
[3] Kas J. *et al.*, *Biophys. J.*, **70** (1996) 609.
[4] Haber C., Ruiz S. A. and Wirtz D., *Proc. Natl. Acad. Sci. U.S.A.*, **97** (2000) 10792.
[5] Onsager L., *Ann. N.Y. Acad. Sci.*, **51** (1949) 627.
[6] Khokhlov A. R. and Semenov A. N., *Physica A*, **108** (1981) 546.
[7] Dogic Z. *et al.*, *Phys. Rev. Lett.*, **92** (2004) 125503.
[8] Van Bruggen M. P. B. *et al.*, *Phys. Rev. E*, **58** (1998) 7668.
[9] Allen M. P., *Phys. Rev. Lett.*, **65** (1990) 2881.
[10] Hess S., Frenkel D. and Allen M. P., *Mol. Phys.*, **74** (1991) 765.
[11] Lowen H., *Phys. Rev. E*, **59** (1989) 1999.
[12] Kruger G. J., *Phys. Rep.*, **82** (1982) 230.
[13] Tang J. and Fraden S., *Liq. Cryst.*, **19** (1995) 459.
[14] Purdy K. R. *et al.*, *Phys. Rev. E*, **67** (2003) 031708.
[15] Cush R. C. and Russo P. S., *Macromolecules*, **35** (2002) 8659.
[16] Dogic Z. and Fraden S., *Philos. Trans. R. Soc. London, Ser. A*, **359** (2001) 997.
[17] Dogic Z. and Fraden S., *Phys. Rev. Lett.*, **78** (1997) 2417.
[18] Dogic Z. and Fraden S., *Langmuir*, **16** (2000) 7820.
[19] Maniatis T., Sambrook J. and Fritsch E. F. E., *Molecular Cloning* (Cold Spring Harbor University Press) 1989.
[20] The code used for tracking particles is available online at the following address: `http://www.physics.emory.edu/~weeks/idl/`.
[21] Addas K. M., Schmidt C. F. and Tang J. X., *Phys. Rev. E*, **70** (2004) 021503.
[22] Islam M/ F. and Yodh A. G., in preparation.